Received March 2002
Revised August 2002
Accepted January 2003

Simulation of viscous 2D-planar cylindrical geometry deformation using DR-BEM

J.P. Hernandez
Department of Mechanical Engineering, Polymer Engineering Center, University of Wisconsin-Madison, Madison, Wisconsin, USA
Energy and Thermodynamic Institute, Universidad Pontificia Bolivariana, Medellin, Colombia
T.A. Osswald
Department of Mechanical Engineering, Polymer Engineering Center, University of Wisconsin-Madison, Madison, Wisconsin, USA
D.A. Weiss
DaimlerChrysler AG, Research and Technology, Ulm, Germany

Keywords *Differential equations, Geometric planes and solids, Boundary elements methods*

Abstract *In this paper, a novel boundary element formulation for the deformation of a viscous 2D-planar cylindrical geometry, immersed in a different viscous fluid and moving towards a rigid wall, is proposed for moderate Reynolds number, considering surface tension effects. The boundary integral formulation for Stokes flow inside and outside the geometry is represented in terms of a combined distribution of a single-layer and a double-layer potential of Green functions over the geometry surface. Additionally, non-linear terms describing effects absent in pure Stokes flow, such as the time derivative of the velocity and inertia, are included. These effects lead to the appearance of domain integrals. Traditional dual reciprocity is applied in order to approximate these domain integrals by a series of particular solutions which are then transformed into boundary integrals. Augmented thin-plate splines, i.e.* $r^2\log(r)$*, plus three additional linear terms from a Pascal triangle expansion were chosen for the dual reciprocity approximation. In order to avoid the discretization of the rigid wall, and using the fact that the velocity on the wall must vanish due to the no-slip condition, the fundamental solution was modified with a combination of image singularities including an image Stokeslet, a potential dipole and a Stokes-doublet.*

International Journal of Numerical Methods for Heat & Fluid Flow
Vol. 13 No. 6, 2003
pp. 698-719

0961-5539
DOI 10.1108/09615530310498385

Introduction

Over the years, boundary integral formulations have been used in order to study the motion of drops and bubbles in pure Stokes flow. Using Green's integral representation formulae for the fluids inside and outside the drop, a second kind Fredholm integral equation is obtained in terms of the velocity and the surface tractions. More details can be found in the works of Power and

Partridge (1994), Power and Wrobel (1995), Pozrikidis (1990, 1992) and Rallison and Acrivos (1978, 1984).

Several numerical techniques have been used to simulate the drop deformation, such as finite differences (Hatta *et al.*, 1995, 1997) and finite volume (Bussmann *et al.*, 1999; Passandideh-Fard *et al.*, 1996). However, these methods require domain discretization. The boundary element method (BEM) offers the great advantage in that it reduces the spatial dimension of the problem by one, expressing the governing equations by boundary-only equations. It has been used in several works to simulate the dynamics of drops in linear problems, like potential flows (Cheng, 2000; Weiss and Yarin, 1999, 1995) and homogeneous Stokes flows (Power and Partridge, 1994; Pozrikidis, 1990, 1992; Primo *et al.*, 2000; Rallison and Acrivos, 1978, 1984).

The BEM has been limited to linear problems because the fundamental solution or Green's function is required to obtain a boundary integral formula equivalent to the original partial differential equation of the problem. The non-homogeneous terms accounting for non-linear effects and body forces were included in the formulation by means of domain integrals, making the method lose its boundary-only character. At present, there are different approaches to overcome these problems. One of the most efficient ones is the dual reciprocity method (DRM), which is the technique used throughout this work to deal with non-linear terms in the momentum equations. The basic idea behind the DRM approach is to approximate the non-homogeneous terms as a series of known functions and in this way obtain a series of particular solutions to the original equation. According to Gomez and Power (1997) the classical DRM works well for Reynolds numbers up to 200. In our applications, such as blending and painting, we will remain at Reynolds number under 200.

In this work, we report on a new formulation that combines the classical BEM equations for drop deformation in Stokes flow, developed and used by Power (1996), Power and Wrobel (1995), Pozrikidis (1990, 1992) and Rallison and Acrivos (1978, 1984), with the DRM, in order to simulate the full Navier-Stokes equations. The proposed model simulates the 2D-planar cylindrical geometry deformation phenomena for moderate Reynolds numbers, and in the presence of a rigid wall and surface tension effects. In the future, this work will be extended to 3D viscous drop deformation. Due to the fact that future formulations will actually deal with 3D geometries a 2D planar cylindrical formulation is more easily transferred when compared to an axis-symmetric formulation.

In the subsequent section, we state the problem. Thus, the governing partial differential equation is transcribed into an integral representation; for the non-linear terms, i.e. the terms describing the deviations from the pure Stokes flow, the DRM is applied. The numerical implementation is described and two cases are tested, and the results are compared with the pure Stokes solution. Finally, the results are interpreted and discussed.

Problem statement

Consider a 2d-planar cylindrical geometry of viscosity μ_2 and density ρ_2, which is immersed in a fluid of viscosity μ_1 and density ρ_1, and which has interfacial surface tension γ. It should be noted that in this formulation μ_1 and μ_2 represent Newtonian viscosities. Figure 1 shows the problem schematically. The governing equations for both the external and internal fluid are the Navier-Stokes equations, rewritten here as follows,

$$\mu_l \frac{\partial^2 u_i}{\partial x_j \partial x_j} - \frac{\partial p}{\partial x_i} = \rho_l \left(\frac{\partial u_i}{\partial t} + u_j \frac{\partial u_i}{\partial x_j} \right) \quad \text{for all } \mathbf{x} \in \Omega_l \tag{1}$$

$$\frac{\partial u_i}{\partial x_i} = 0 \tag{2}$$

where $l = 1, 2$ represent the external and internal fluid, respectively, $\mathbf{u}$ is the velocity field, p the pressure or the modified pressure, depending on if the gravity is included or not in the analysis, and $\Omega = \Omega_1 + \Omega_2$ a planar two-dimensional domain.

The flow field has to satisfy the following boundary conditions,

$$u_i = 0 \quad \text{for all } \mathbf{x} \in \text{Wall} \tag{3}$$

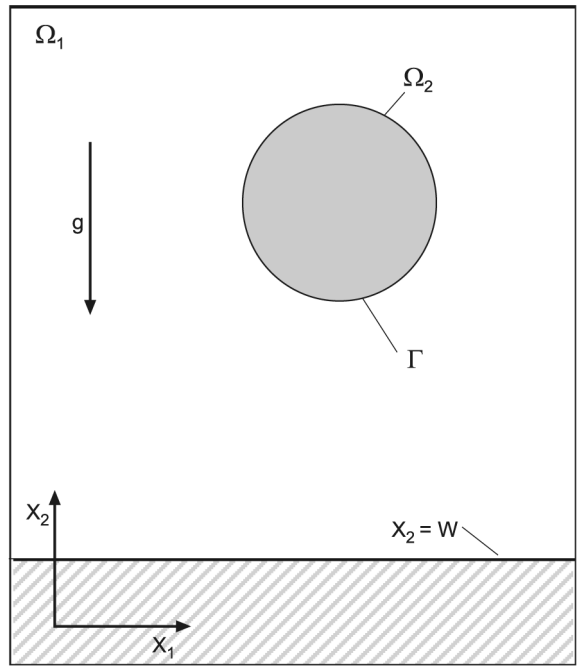

Figure 1.
Problem schematic

$$[u_i]_\Gamma = 0 \tag{4}$$

$$[\sigma_{ij} n_j]_\Gamma = \phi \rho_1 (\beta - 1) g_i + \gamma k n_i \qquad \text{for all } \mathbf{x} \notin \text{Wall} \tag{5}$$

where $[]_\Gamma$ denotes the jump across the surface Γ from outside Ω_1 to the inside Ω_2, $\boldsymbol{n}$ is the outward normal unit vector, k is the surface curvature, ϕ defines the presence of the gravity field with values 0 or 1, $\mathbf{g}$ is the gravity field, β is the density ratio defined as $\beta = \rho_2/\rho_1$ and σ_{ij} the stress tensor defined as,

$$\sigma_{ij} = -p\delta_{ij} + \mu_l \left(\frac{\partial u_i}{\partial x_j} + \frac{\partial u_j}{\partial x_i} \right) \tag{6}$$

where δ_{ij} denotes the Kronecker delta function.

Integral formulation and the DRM

The integral representation formulae for the velocity fields are found from Green's formulae for Stokes equations given by Ladyzhenskaya (1963). In the exterior problem it will be,

$$u_i(\mathbf{x}_0) - \int_\Gamma K_{ij}(\mathbf{x}, \mathbf{x}_0)(u_j(\mathbf{x}))_1 \, \mathrm{d}\Gamma = -\frac{1}{\mu_1} \int_\Gamma u_i^j(\mathbf{x}, \mathbf{x}_0)(\sigma_{jk}(\mathbf{u}(\mathbf{x})))_1 n_k(\mathbf{x}) \, \mathrm{d}\Gamma + \frac{1}{\mu_1} \int_{\Omega_1} u_i^j(\mathbf{x}, \mathbf{x}_0) d_j^1(\mathbf{x}) \, \mathrm{d}\Omega \tag{7}$$

for every $\mathbf{x} \in \Omega_1$, where $(\mathbf{u}(\mathbf{x}))_1$ and $(\sigma_{ij}(\mathbf{u}(\mathbf{x})))_1$ are the values of the velocity field $\mathbf{u}$ and of the stress $\sigma_{ij}(\mathbf{u}(\mathbf{x}))$, respectively, at a point $\mathbf{x} \in \Gamma$ coming from Ω_1.

For the fluid in the drop, the Green's representation formulae is given by,

$$u_i(\mathbf{x}_0) + \int_\Gamma K_{ij}(\mathbf{x}, \mathbf{x}_0)(u_j(\mathbf{x}))_2 \, \mathrm{d}\Gamma = \frac{1}{\mu_2} \int_\Gamma u_i^j(\mathbf{x}, \mathbf{x}_0)(\sigma_{jk}(\mathbf{u}(\mathbf{x})))_2 n_k(\mathbf{x}) \, \mathrm{d}\Gamma + \frac{1}{\mu_2} \int_{\Omega_2} u_i^j(\mathbf{x}, \mathbf{x}_0) d_j^2(\mathbf{x}) \, \mathrm{d}\Omega \tag{8}$$

for every $\mathbf{x} \in \Omega_2$, where $(\mathbf{u}(\mathbf{x}))_2$ and $(\sigma_{ij}(\mathbf{u}(\mathbf{x})))_2$ are the values of the velocity field $\mathbf{u}$ and of the stress $\sigma_{ij}(\mathbf{u}(\mathbf{x}))$, respectively, at a point $\mathbf{x} \in \Gamma$ coming from Ω_2.

For equations (7) and (8) $\mathbf{d}^l$ is the non-homogeneous term or pseudo-body force defined as follows,

$$d_i^l = \rho_l \left(\frac{\partial u_i}{\partial t} + u_j \frac{\partial u_i}{\partial x_j} \right) \tag{9}$$

Assuming that the densities of both fluids are constant, the non-linear terms can be normalized with respect to the densities, i.e.

$$d_i^l = \rho_l d_i \qquad \text{for } l = 1, 2 \tag{10}$$

From condition (4) it can be concluded that $(\mathbf{u}(\mathbf{x}))_1 = (\mathbf{u}(\mathbf{x}))_2 = \mathbf{u}(\mathbf{x})$, for every point $\mathbf{x} \in \Gamma$. Letting a point $\mathbf{x} \in \Omega_1$ approach a point $\xi \in \Gamma$, equation (7) changes to,

$$c_{ij}^1 u_i(\mathbf{x}_0) - \int_\Gamma K_{ij}(\mathbf{x}, \mathbf{x}_0) u_j(\mathbf{x})\, d\Gamma = -\frac{1}{\mu_1}\int_\Gamma u_i^j(\mathbf{x}, \mathbf{x}_0)(\sigma_{jk}(\mathbf{u}(\mathbf{x})))_1 n_k(\mathbf{x})\, d\Gamma + \frac{1}{\mu_1}\int_{\Omega_1} u_i^j(\mathbf{x}, \mathbf{x}_0) d_j^1(\mathbf{x})\, d\Omega \tag{11}$$

In the same way, letting a point $\mathbf{x} \in \Omega_2$ approach a point $\xi \in \Gamma$, equation (8) will be,

$$c_{ij}^2 u_i(\mathbf{x}_0) + \int_\Gamma K_{ij}(\mathbf{x}, \mathbf{x}_0) u_j(\mathbf{x})\, d\Gamma = \frac{1}{\mu_2}\int_\Gamma u_i^j(\mathbf{x}, \mathbf{x}_0)(\sigma_{jk}(\mathbf{u}(\mathbf{x})))_2 n_k(\mathbf{x})\, d\Gamma + \frac{1}{\mu_2}\int_{\Omega_2} u_i^j(\mathbf{x}, \mathbf{x}_0) d_j^2(\mathbf{x})\, d\Omega \tag{12}$$

The coefficients c_{ij}^1 and c_{ij}^2 depend on the shape of the surface Γ around the point $\mathbf{x}$. If Γ is smooth in $\mathbf{x}$, both the coefficients are equal to $\delta_{ij}/2$. In the present work, the surface was assumed to be smooth during deformation, then the assumption can be acceptable also for the contact point, between the internal fluid, external fluid and the wall, when the wetting angle is π. In a more general formulation, the coefficient for this contact point can be found using the wetting angle as follows (Pozrikidis, 1992),

$$c_{ij} = \frac{\theta}{2\pi} \tag{13}$$

where θ is the wetting angle.

In order to express the domain integral in equations (11) and (12) into equivalent boundary integrals several methods have been developed (Cheng, 2000; Florez, 2000; Goldberg and Chen, 1997; Liao, 1997; Power and Mingo, 2000). The dual reciprocity approximation introduced by Nardini and Brebbia (1982) is one such method, where the basic idea is to expand the non-homogeneous terms or pseudo-body forces as a series of known interpolation functions. Several types of non-linearities can be approximated with this method, such as non-Newtonian fluids (Davis, 1995; Davis and Osswald, 1995; Florez, 2000; Hernandez, 1999; Rios, 1999), full Navier-Stokes

equations (Florez, 2000; Florez and Power, 2001; Florez *et al.*, 2000; Power and Mingo, 2000) and transient problems (Power, 1993). Full details of the dual reciprocity approximation can be found in the work of Wrobel and Brebbia (1987) or Partridge *et al.* (1991). A brief description of the method starts with the expansion of the non-linear term **d** using radial or global interpolation functions, i.e.

$$d_i(\mathbf{x}) = \sum_{m=1}^{N+A} f(\mathbf{x}, \mathbf{x}^m)\alpha_l^m \delta_{il} \tag{14}$$

The coefficients of α_l^m are unknown terms, which can be solved for by the application of equation (14) at each of the collocation nodes located on both the boundary, and the internal and external domain, where the non-linear terms are approximated. The functions $f(\mathbf{x},\mathbf{x}^m)$ depend only on geometry. There are two types, radial basis functions and global functions. It will be considered here that in addition to the radial basis functions there are $A = 3$ augmentation global functions from the set $\{1,x_1,x_2\}$, arriving to the so-called augmented spline, which consists of the radial basis function plus a series of additional global functions (Goldberg and Chen, 1996, 1997). As pointed out by Partridge (2000) there are criteria for selecting the type of the approximation functions. The radial basis function used in this work is the thin-plate spline (TPS),

$$f(\mathbf{x}, \mathbf{x}^m) = r^2 \log(r) \tag{15}$$

where $r = r(\mathbf{x}, \mathbf{x}^m)$ is the Euclidean distance between the field point **x** and the collocation point $\mathbf{x}^m$. Equation (14) when applied to the N collocation nodes generates $2N$ linear equations with $2(N+A)$ unknowns and therefore $2A$ additional conditions are necessary which basically guarantee maximum smoothness of the interpolant (Florez, 2000; Goldberg and Chen, 1996, 1997). These additional relationships are expressed as,

$$\sum_{j=1}^{N} \alpha_l^j \delta_{il} = \sum_{j=1}^{N} x_1^j \alpha_l^j \delta_{il} = \sum_{j=1}^{N} x_2^j \alpha_l^j \delta_{il} = 0 \tag{16}$$

where $\mathbf{x}^j$ represents the jth collocation node.

With the approximation given in equation (14), the domain integral in equations (11) and (12) becomes,

$$\int_\Omega u_i^j(\mathbf{x}, \mathbf{x}_0) d_i(\mathbf{x})\, \mathrm{d}\Omega = \sum_{j=1}^{N+A} \alpha_l^m \int_\Omega u_i^j(\mathbf{x}, \mathbf{x}_0) f(\mathbf{x}, \mathbf{x}^m) \delta_{il}\, \mathrm{d}\Omega \tag{17}$$

To reduce the last domain integral to a boundary integral, a new auxiliary non-homogeneous Stokes' field is defined for each interpolation function as follows,

$$\mu \frac{\partial^2 \hat{u}_i^{lm}(\mathbf{x})}{\partial x_j \partial x_j} - \frac{\partial \hat{p}^{lm}(\mathbf{x})}{\partial x_i} = f^m(\mathbf{x})\delta_{il} \tag{18}$$

$$\frac{\partial \hat{u}_i^{lm}}{\partial x_i} = 0 \tag{19}$$

where $\hat{u}_i^{lm}$ is the auxiliary non-homogeneous velocity field with the corresponding pressure $\hat{p}^{lm}$. Applying Green's identities to the flow field $\left(\hat{u}_i^{lm}(\mathbf{x}), \hat{p}^{lm}(\mathbf{x})\right)$ and substituting the resulting domain integrals into equations (11) and (12), the following boundary-only integral formulae for the velocity field is obtained,

$$\begin{aligned}
&\frac{1}{2}u_i(\mathbf{x}_0) - \int_\Gamma K_{ij}(\mathbf{x}, \mathbf{x}_0) u_j(\mathbf{x})\, \mathrm{d}\Gamma + \frac{1}{\mu_1}\int_\Gamma u_i^j(\mathbf{x}, \mathbf{x}_0)(\sigma_{ij}(\mathbf{u}(\mathbf{x})))_1 n_j(\mathbf{x})_\Gamma\, \mathrm{d}\Gamma \\
&\quad = \sum_{m=1}^{N+A} \frac{\rho_1}{\mu_1}\alpha^m \left\{ \frac{1}{2}\hat{u}_j^{lm}(\mathbf{x}) - \int_\Gamma K_{ij}(\mathbf{x}, \mathbf{x}_0)\hat{u}_j^{lm}(\mathbf{x}, \mathbf{x}^m)\, \mathrm{d}\Gamma \right. \\
&\quad \left. - \int_\Gamma u_i^j(\mathbf{x}, \mathbf{x}_0)\hat{t}_j^{lm}(\mathbf{x}, \mathbf{x}^m)\, \mathrm{d}\Gamma \right\}
\end{aligned} \tag{20}$$

$$\begin{aligned}
&\frac{1}{2}u_i(\mathbf{x}_0) + \int_\Gamma K_{ij}(\mathbf{x}, \mathbf{x}_0) u_j(\mathbf{x})\, \mathrm{d}\Gamma - \frac{1}{\mu_2}\int_\Gamma u_i^j(\mathbf{x}, \mathbf{x}_0)(\sigma_{ij}(\mathbf{u}(\mathbf{x})))_2 n_j(\mathbf{x})_\Gamma\, \mathrm{d}\Gamma \\
&\quad = \sum_{m=1}^{N+A} \frac{\rho_2}{\mu_2}\alpha^m \left\{ \frac{1}{2}\hat{u}_j^{lm}(\mathbf{x}) + \int_\Gamma K_{ij}(\mathbf{x}, \mathbf{x}_0)\hat{u}_j^{lm}(\mathbf{x}, \mathbf{x}^m)\, \mathrm{d}\Gamma \right. \\
&\quad \left. - \int_\Gamma u_i^j(\mathbf{x}, \mathbf{x}_0)\hat{t}_j^{lm}(\mathbf{x}, \mathbf{x}^m)\, \mathrm{d}\Gamma \right\}
\end{aligned} \tag{21}$$

The analytical expression for the auxiliary Stokes flow field $\left(\hat{u}_i^{lm}(\mathbf{x}), \hat{p}^{lm}(\mathbf{x})\right)$ corresponding to the TPS interpolation can be found by the approach suggested by Power and Wrobel (1995). They are developed and listed in Appendix. The particular solution for velocity, inside or outside, are identical, since the equations were normalized using the density according to equation (10). However, the traction particular solutions are of opposite sign, due to the direction of the normal vector.

Multiplying equation (21) by $\lambda = \mu_2/\mu_1$, and adding to equation (20) gives,

$$\frac{1}{2}u_i(\mathbf{x}_0) - a_1\int_\Gamma K_{ij}(\mathbf{x},\mathbf{x}_0)u_j(\mathbf{x})\,d\Gamma + a_2\int_\Gamma u_i^j(\mathbf{x},\mathbf{x}_0)\left[\sigma_{ij}(\mathbf{u}(\mathbf{x}))n_j(\mathbf{x})\right]_\Gamma d\Gamma$$

$$= a_4\sum_{m=1}^{N+A}\alpha^m\left\{\frac{1}{2}\hat{u}_j^{lm}(\mathbf{x}) - a_3\int_\Gamma K_{ij}(\mathbf{x},\mathbf{x}_0)\hat{u}_j^{lm}(\mathbf{x},\mathbf{x}^m)\,d\Gamma\right. \tag{22}$$

$$\left. - \int_\Gamma u_i^j(\mathbf{x},\mathbf{x}_0)\hat{t}_j^{lm}(\mathbf{x},\mathbf{x}^m)\,d\Gamma\right\}$$

where,

$$a_1 = \frac{(1-\lambda)}{(1+\lambda)}, \quad a_2 = \frac{1}{(\lambda+1)\mu_1}, \quad a_3 = \frac{(1-\beta)}{(1+\beta)}, \quad a_4 = \frac{(\beta+1)\rho_1}{(\lambda+1)\mu_1}. \tag{23}$$

Similarly, Power and Wrobel (1995), Pozrikidis (1990) and Rallison and Acrivos (1978) found a second kind Fredholm integral similar to equation (22). The parameter of the Fredholm equation is the same and equal to a_1, but the free or non-homogeneous term does not include the dual reciprocity approximation given in equation (22). In fact, this is the additional term that completes the new formulation proposed in this paper.

Without the influence of the rigid wall, Green's function u_i^k under the second integral in equation (22) is the fundamental solution of Stokes' equation known as *Stokeslet*, with a corresponding pressure q^k. For planar two-dimensional problems they are defined as,

$$u_i^k(x) = \left(-\ln(r)\delta_{ik} + \frac{x_i x_k}{r^2}\right) \tag{24}$$

$$q^k(\mathbf{x}) = -\frac{1}{2\pi}\frac{x_k}{r^2} \tag{25}$$

and K_{ij} represents the traction fundamental solution given by

$$K_{ij}(\mathbf{x}) = -4\frac{x_i x_j x_k}{r^4}n_k(\mathbf{x}) \tag{26}$$

Blake (1971) and Pozrikidis (1990, 1992) showed that in the presence of the rigid wall in $x_2 = w$, $u_i^j(\mathbf{x})$ may be expressed in terms of a Stokeslet, and a finite collection of image singularities including an image Stokeslet, a potential dipole and a Stokes-doublet,

$${}^{\mathrm{w}}u_i^j(\mathbf{x},\mathbf{x}_0) = \frac{1}{4\pi}\left(u_i^j(\hat{\mathbf{x}}) - u_i^j(\tilde{\mathbf{x}}) + 2h^2U_{ij}^{\mathrm{D}}(\tilde{\mathbf{x}}) - 2hU_{ij}^{\mathrm{SD}}(\tilde{\mathbf{x}})\right) \tag{27}$$

where $h = x_{2,0} - w$ is the distance of the point from the wall, $\hat{\mathbf{x}} = \mathbf{x} - \mathbf{x}_0$, $\tilde{\mathbf{x}} = \mathbf{x} - \mathbf{x}_0^{\text{im}}$, and $\mathbf{x}_0^{\text{im}} = (x_{1,0}, 2w - x_{2,0})$ is the image of $\mathbf{x}_0$ with respect to the wall. The tensors $\mathbf{U}^{\text{D}}$ and $\mathbf{U}^{\text{SD}}$ represent potential dipoles and Stokes doublets. For two-dimensional planar domains, they are defined as,

$$U_{ij}^{\text{D}}(\mathbf{x}) = \pm \frac{\partial}{\partial x_j}\left(\frac{x_i}{r^2}\right) = \pm\left(\frac{\delta_{ij}}{r^2} - 2\frac{x_i x_j}{r^4}\right) \tag{28}$$

$$U_{ij}^{\text{SD}}(\mathbf{x}) = \pm \frac{\partial u_i^2}{\partial x_j} = x_2 U_{ij}^{\text{D}}(\mathbf{x}) \pm \frac{\delta_{j_2} x_i - \delta_{i_2} x_j}{r^2} \tag{29}$$

with a plus sign for $j = 1$, in the x_1 direction, and a minus sign for $j = 2$ in the x_2 direction. The associated pressure vector is given by,

$${}^{\text{w}}q^i(\mathbf{x}, \mathbf{x}_0) = q^i(\hat{\mathbf{x}}) - q^i(\tilde{\mathbf{x}}) - 2hq_{\text{SD}}^j(\tilde{\mathbf{x}}) \tag{30}$$

where

$$q_{\text{SD}}^j(\mathbf{x}) = -\frac{2}{r^4}(2x_1x_2, x_1^2 - x_2^2) \tag{31}$$

The associated stress tensor is given by

$${}^{\text{w}}T_{ijk}(\mathbf{x}, \mathbf{x}_0) = \frac{1}{4\pi}\left(T_{ijk}(\hat{\mathbf{x}}) - T_{ijk}(\tilde{\mathbf{x}}) + 2h^2 T_{ijk}^{\text{D}}(\tilde{\mathbf{x}}) - 2hT_{ijk}^{\text{SD}}(\tilde{\mathbf{x}})\right) \tag{32}$$

The tensors $\mathbf{T}^{\text{D}}$ and $\mathbf{T}^{\text{SD}}$ may be computed by straightforward differentiation using the following equations,

$$T_{ijk}^{\text{D}} = \frac{\partial U_{ij}^{\text{D}}}{\partial x_k} + \frac{\partial U_{kj}^{\text{D}}}{\partial x_i} \tag{33}$$

$$T_{ijk}^{\text{SD}} = -\delta_{ik}q^j + \frac{\partial U_{ij}^{\text{SD}}}{\partial x_k} + \frac{\partial U_{kj}^{\text{SD}}}{\partial x_i} \tag{34}$$

Numerical implementation

For the numerical solution of equation (22) the surface of the geometry was divided into smaller quadratic elements. Each element has three nodes and equation (22) is applied to each node of every element. For the external or internal points, equations (11) and (12) are applied, respectively. The surface integrals that appear on those equations can be evaluated numerically using Gauss-Legendre quadratures (Florez, 2000; Hernandez, 1999; Partridge, 1997). However, special attention should be paid to the weakly singular integrals

whose kernel is the Stokeslet $u_i^j(\mathbf{x}, \mathbf{x}_0)$ when the source point tends to the field point. This singularity can be dealt with by using a special coordinate transformation (Telles, 1987).

After applying the dual reciprocity on each node and evaluating the boundary integrals of the quadratic boundary elements, the following matrix system is obtained

$$\frac{1}{2}\mathbf{u} - a_1\bar{\mathbf{H}}\mathbf{u} + a_2\mathbf{G}\mathbf{t} = a_4\left[\frac{1}{2}\hat{\mathbf{U}} - a_3\bar{\mathbf{H}}\hat{\mathbf{U}} - \mathbf{G}\hat{\mathbf{T}}\right]\boldsymbol{\alpha} \tag{35}$$

where $\bar{\mathbf{H}}$ and $\mathbf{G}$ are square matrices whose entries are integrals of the product of the corresponding kernel (${}^{\mathrm{w}}u_i^j(\mathbf{x}, \mathbf{x}_0)$ and ${}^{\mathrm{w}}K_{ij}(\mathbf{x}, \mathbf{x}_0) = {}^{\mathrm{w}}T_{ijk}(\mathbf{x}, \mathbf{x}_0)n_k(\mathbf{x})$) by the shape functions that are used to interpolate along the boundary elements (Brebbia and Dominguez, 1989; Brebbia *et al.*, 1984). Vectors $\mathbf{u}$ and $\mathbf{t}$ are the velocities and tractions, respectively; $\hat{\mathbf{U}}$ and $\hat{\mathbf{T}}$ are matrices whose columns correspond to the particular solution of the auxiliary Stokes problem, and the constants $a_i (i = 1, \ldots, 4)$ are defined in equation (23). After some mathematical manipulation equation (34) can be organized as follows,

$$\mathbf{H}\mathbf{u} - \mathbf{G}\mathbf{t} = \left[\mathbf{H}_\mathbf{d}\hat{\mathbf{U}} - \mathbf{G}_\mathbf{d}\hat{\mathbf{T}}\right]\boldsymbol{\alpha} \tag{36}$$

The unknown coefficient vector $\boldsymbol{\alpha}$ is determined from equation (14). Using the traditional dual reciprocity to approximate the derivatives of the velocity (Hernandez, 1999; Partridge *et al.*, 1991; Power and Wrobel, 1995), the unknown coefficient vector becomes,

$$\boldsymbol{\alpha} = \mathbf{F}^{-1}\left[\frac{\partial \mathbf{u}}{\partial t} + \left(u_j\frac{\partial \mathbf{F}}{\partial x_j}\mathbf{F}^{-1}\right)\mathbf{u}\right] \tag{37}$$

For the time derivative in equation (37), a first order explicit time integration scheme is employed. A linear approximation can be proposed for u_i within each time-step in the form,

$$\frac{\partial u_i}{\partial t} = \frac{1}{\mathrm{d}t}\left(u_i^{m+1} - u_i^m\right) \tag{38}$$

Due to the fact that in the present problem there are moving boundaries, all the matrices in equations (36) and (37), which depend on the geometry, vary in time. Thus, equation (37), with (38) will be,

$$\mathbf{S}^m(\mathbf{u}^{m+1} - \mathbf{u}^m) = \mathrm{d}t\left\{(\mathbf{H}\mathbf{u} - \mathbf{G}\mathbf{t}) - \mathbf{S}\left(\left(\mathbf{u}^\mathbf{j}\frac{\partial \mathbf{F}}{\partial \mathbf{x}_\mathbf{j}}\mathbf{F}^{-1}\right)\mathbf{u}\right)\right\}^m \tag{39}$$

where

$$\mathbf{S} = \left[\mathbf{H}_\mathrm{d}\hat{\mathbf{U}} - \mathbf{G}_\mathrm{d}\hat{\mathbf{T}}\right]\mathbf{F}^{-1} \tag{40}$$

The rate of deformation of the drop is determined by the kinematic boundary condition, which states that the normal component of the fluid velocity at any point of the drop's surface is equal to the normal component of the surface velocity at that point,

$$\frac{\mathrm{d}x_i}{\mathrm{d}t} n_i = u_i n_i \tag{41}$$

Thus, for each time step the initial conditions are known, and with equation (41) the coordinates are changed, and the matrices in equation (39) are calculated. If the boundary node is not on the wall, the unknowns for the next time-step are the velocities, and the tractions are calculated with the surface tension coefficient and the curvature of the drop. Once the boundary node touches the wall, the velocities are known, and the tractions are found.

With the use of equation (41) when solving the Navier-Stokes equation, continuity is not fully satisfied since a point will inevitably leave its path during advancement. To correct this problem the advancement of the surfaces must be done iteratively using equation (41) and continuity.

In order to calculate the curvature of the drop in each point and for each time-step Primo *et al.* (2000) implemented a simple procedure. The curvature and normal vector are calculated by fitting a fourth-order Lagrangian polynomial. Five nodal points are taken for the fitting, two to each side of the centre node. The normal and the curvatures are then calculated from the expressions,

$$n_i(x^c) = \frac{1}{\sqrt{\left(x'_1\right)^2 + \left(x'_2\right)^2}} \begin{pmatrix} x'_2 \\ -x'_1 \end{pmatrix} \tag{42}$$

$$k(x^c) = \frac{x'_1 x''_2 - x'_2 x''_1}{\left(\left(x'_1\right)^2 + \left(x'_2\right)^2\right)^{3/2}} \tag{43}$$

where

$$x'_i(x^c) = \frac{1}{6}\left(x_i^{c-2} - 8x_i^{c-1} + 8x_i^{c+1} - x_i^{c+2}\right) \tag{44}$$

and

$$x''_i(x^c) = \frac{1}{3}\left(-x_i^{c-2} + 16x_i^{c-1} - 30x_i^c + 16x_i^{c+1} - x_i^{c+2}\right) \tag{45}$$

whose superscripts indicate the position of the node relative to the centre node, c.

Results

The calculations of the numerical examples presented in this paper were obtained on an IBM compatible computer with two 2.0 GHz Pentium III processors and 1.0 GB RAM. The number of Gauss points taken for the numerical integration was 20. A mesh of 40 nodes and 41 internal nodes was used (Figure 2). Typical computational times for the above parameters were of the order of 1.0 min for 100 time steps.

Recovery due to surface tension effects

A simple way to check the new formulation qualitatively is to verify if the geometry, when starting from an elliptical shape and under negligible gravity effects ($\phi = 0$) and initial velocity, recovers its circular shape due to surface tension.

Figure 3 shows the recovery for the Navier-Stokes case compared to the recovery of the drop for the pure stokes flow. The viscosity for the internal fluid was chosen as 1.0×10^3 pa s and the internal density was 1.0×10^3 kg/m^3, while for the external flow the viscosity was 1.0×10^{-6} pa s and the density was 1.0×10^{-6} kg/m^3. These values in conjunction with a typical value for the recovery velocity, 0.01 m/s, and an average drop diameter, 0.001 m, *will* result in a Reynolds number of 0.0001 for the internal fluid and 10 for the external fluid. The surface tension was chosen as 0.01 N/m.

Inertia terms are not included in pure Stokes, and the circular geometry is obtained and the velocities go to zero. For the initial steps of the recovery

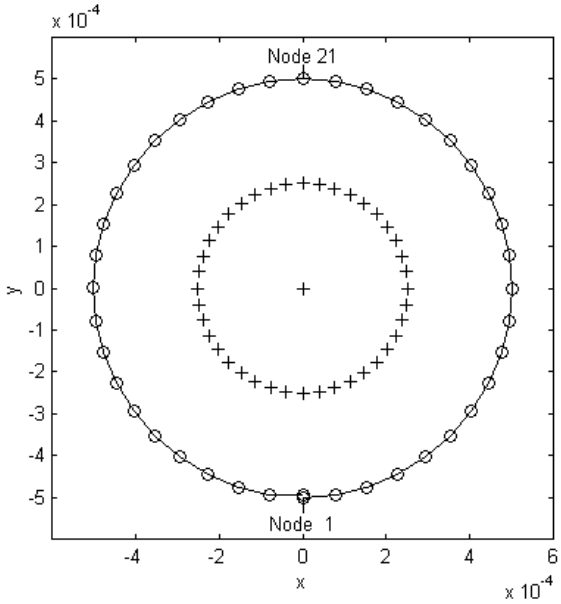

Figure 2.
Drop discretization, surface and internal nodes

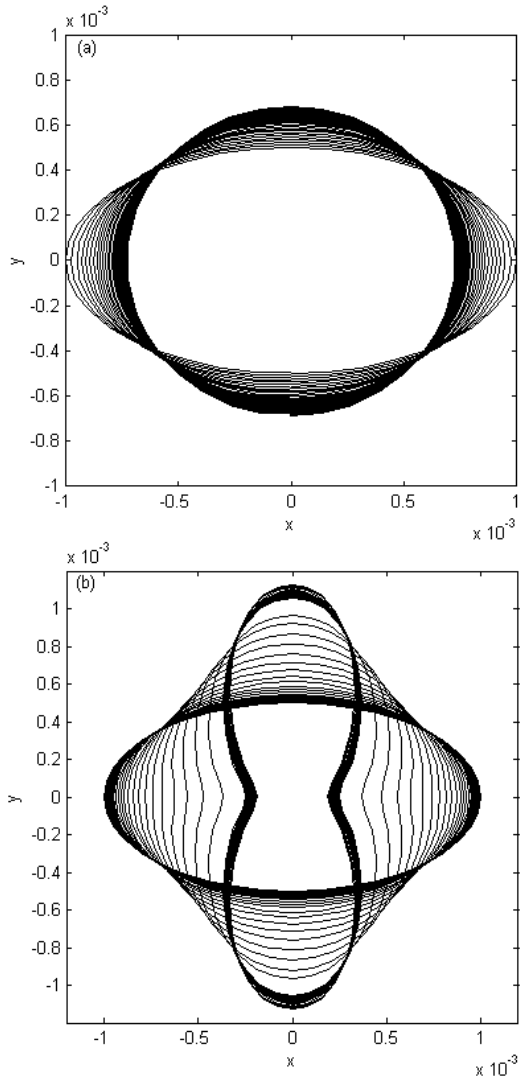

Figure 3.
Geometry change for the recovery: (a) pure Stokes, and (b) Navier-Stokes

the velocity reaches the maximum value. In the case of Navier-Stokes the inertia effects create oscillations, the velocities start from zero, then reach the maximum value and when the geometry passes the circular shape the velocities change direction. The time derivative included in the present paper also causes significant differences between the solutions. At the initial condition the velocities are zero, then the geometry increases velocity. For the pure stokes case this accelerating effect is not considered (Figures 4 and 5), and the velocities start from a higher value and decrease until zero.

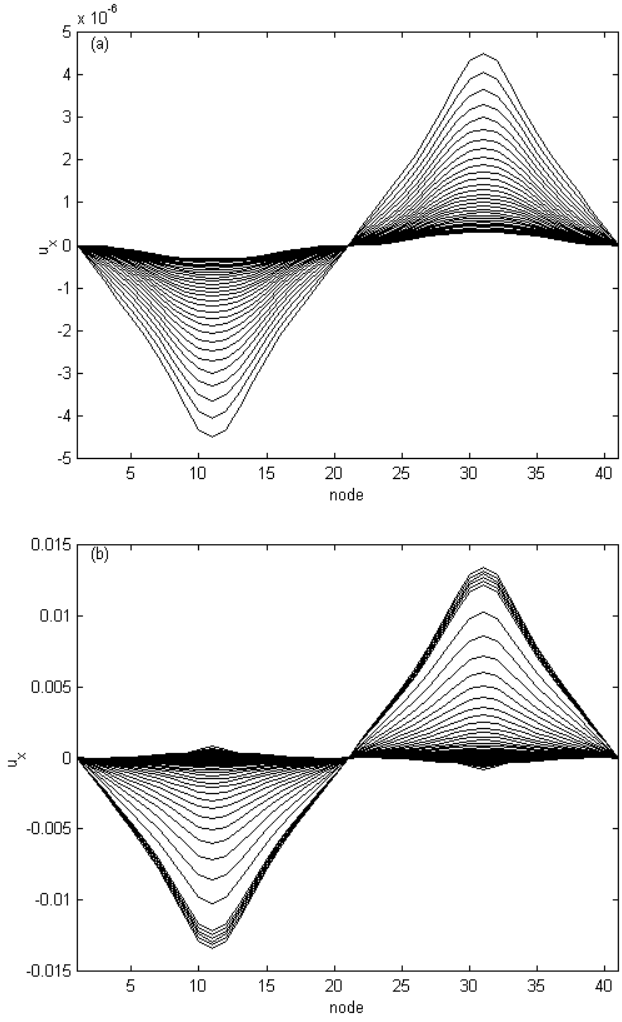

Figure 4.
Velocities in the x-direction for the recovery case: (a) pure stokes, and (b) Navier-Stokes

For the Navier-Stokes case, the velocities start from zero and increase and decrease during the oscillation.

Finally, Figure 6 shows how the drop recovery can be reduced by increasing the viscosity (1.0×10^4 Pa s) of the internal fluid or by decreasing its density (1.0×10^2 kg/m^3). In other words, by increasing the viscous effects or by decreasing the inertia effects.

Motion towards the rigid wall

The second way to check the formulation is simulating the motion of the drop towards a rigid wall in a gravity field, starting from a circular shape and with

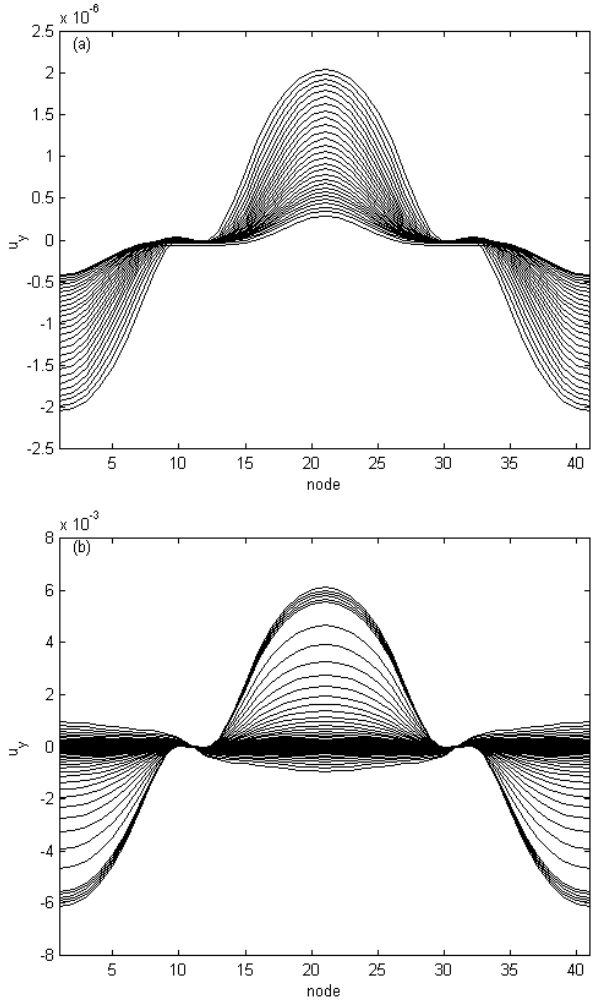

Figure 5.
Velocities in the *y*-direction for the recovery case: (a) pure Stokes, and (b) Navier-Stokes

zero velocity. The viscosity for the internal fluid was chosen as 1.0×10^3 Pa s and the internal density was 1.0×10^3 kg/m^3, while for the external flow the viscosity was 1.0×10^{-6} Pa s and the density was 1.0×10^0 kg/m^3, which represent an internal Reynolds number of 0.001 and an external Reynolds number of 100. The gravity was set to 1.0e1 m/s^2, surface tension to 0.01 N/m and the time step to 1.0×10^{-2} s. In Figure 7 the pure Stokes and the Navier-Stokes solution are compared. In the case of pure Stokes the motion is faster at the beginning and at the end the geometry is far from the wall. The external fluid near the wall has zero velocity and considering only viscous effects the geometry will arrive at stagnation points. In the Navier-Stokes

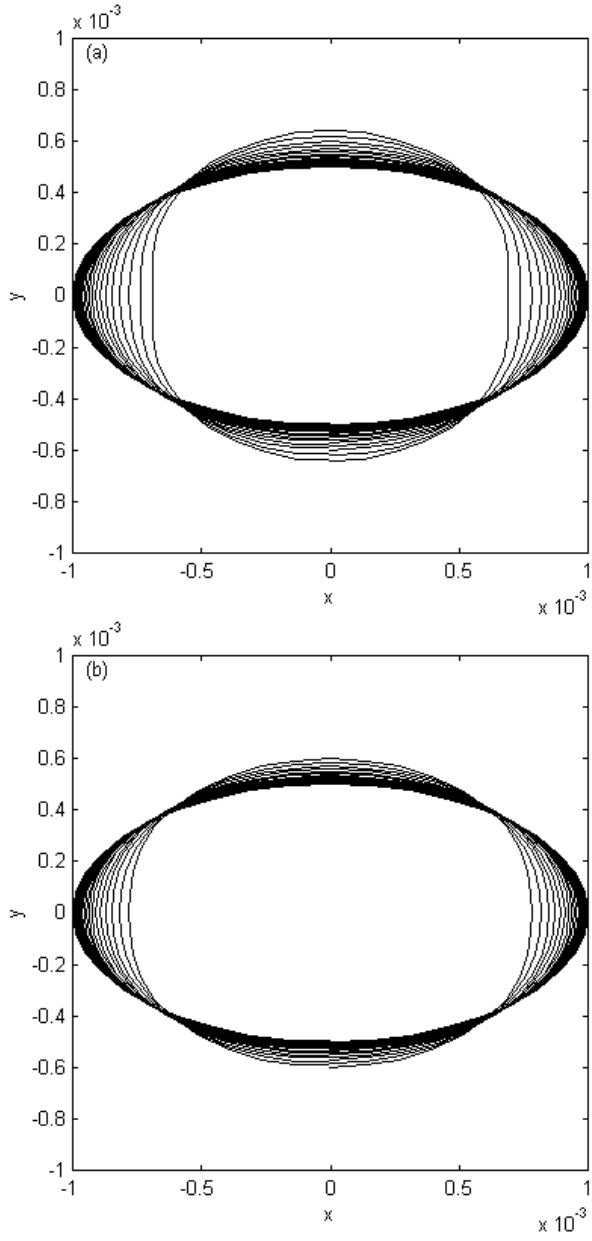

Figure 6.
Navier-Stokes solution for different internal properties: (a) high viscosity, and (b) low density

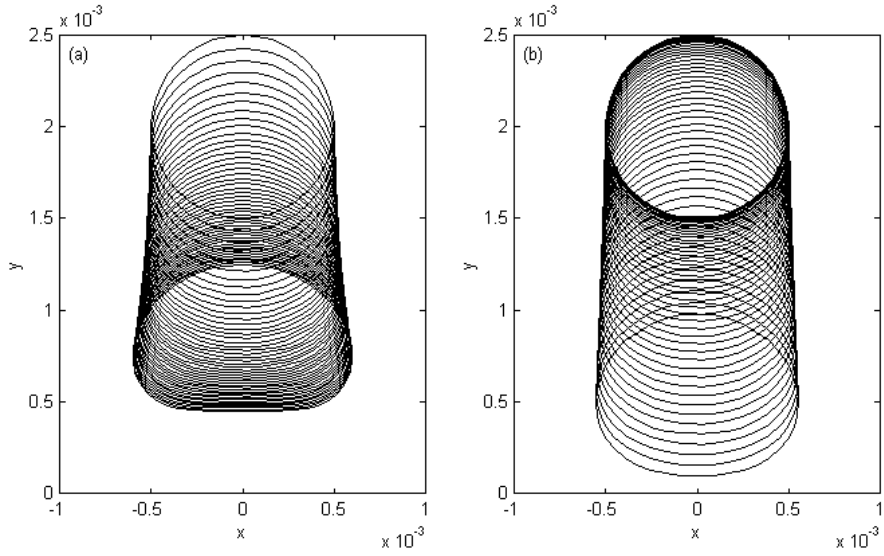

Figure 7.
Motion towards the rigid wall in gravity field: (a) pure Stokes, and (b) Navier-Stokes

solution the geometry accelerates at the beginning and at the end is closer to the wall, due to the inertia terms. The final shapes also present some differences. In pure Stokes flow the geometry is flat at the bottom, while in the Navier-Stokes solution the geometry still has a circular shape.

Conclusion

The new formulation, combining the boundary element classical approach for the deformation of drops and the DRM was satisfactorily tested in to simple cases and compared with the pure Stokes solution. Recovery under surface tension effects and the motion towards a rigid wall in a gravity field were the cases that help to prove that the new formulation can be used to include time derivative and inertia effects at moderate Reynolds numbers.

References

Blake, J.R. (1971), "A note on the imagine system for a Stokeslet in a no-slip boundary", *Proc. Camb. Phil. Soc.*, Vol. 70, pp. 303-10.

Brebbia, C.A. and Dominguez, J. (1989), *Boundary Elements, An Introductory Course*, Computational Mechanics Publications, Southampton.

Brebbia, C.A., Telles, J.C.F. and Wrobel, L.C. (1984), *Boundary Elements Techniques*, Springer-Verlag, New York.

Bussmann, M., Mostaghimi, J. and Chandra, S. (1999), "On a three-dimensional volume tracking model of droplet impact", *Physics of Fluids*, Vol. 11 No. 6, pp. 1406-17.

Cheng, A. (2000), "Particular solutions of Laplacian, Helmholtz-type, and polyharmonic operators involving higher order radial basis functions", *Eng. Anal. Bound. Elem.*, Vol. 24, pp. 539-47.

Cheng, A., Lafe, O. and Grilli, S. (1994), "Dual reciprocity BEM based on global interpolation functions", *Eng. Anal. Bound. Elem.*, Vol. 13, pp. 303-11.

Davis, B.A. (1995), "Investigation of non-linear flows in polymer mixing using the boundary integral method", PhD thesis, Mechanical Engineering Department, University of Wisconsin-Madison, USA.

Davis, B.A. and Osswald, T.A. (1995), "A non-Newtonian simulation method for moving boundary problems using DRM-BEM", *BEM XVII*, Computational Mechanics Publications, New York, pp. 541-8.

Florez, W.F. (2000), "Multidomain dual reciprocity method for the solution of nonlinear flow problems", PhD thesis, University of Wales, Wessex Institute of Technology, Southtampton.

Florez, W.F. and Power, H. (2001), "Comparison between continuous and discontinuous boundary elements in the multidomain dual reciprocity method for the solution of the two-dimensional Navier-Stokes equations", *Eng. Anal. Bound. Elem.*, Vol. 25, pp. 57-69.

Florez, W.F., Power, H. and Chejne, F. (2000), "Multi-domain dual reciprocity BEM approach for the Navier-Stokes system of equations", *Commun. Numer. Meth. Eng.*, Vol. 16, pp. 671-81.

Goldberg, M.A. and Chen, C.S. (1996), "A bibliography on radial basis function approximation", *Boundary Elements Communications*, Vol. 7 No. 4, pp. 155-64.

Goldberg, M.A. and Chen, C.S. (1997), *Discrete Projection Methods for Integral Equations*, Computational Mechanics Publications, Southampton.

Gomez, J.E. and Power, H. (1997), "A multipole direct and indirect BEM for 2D cavity flow at low Reynolds number", *Eng. Anal. Bound. Elem.*, Vol. 19, pp. 17-31.

Happel, J. and Brenner, H. (1973), *Low Reynolds Number Hydrodynamics*, Matinus noordhoff, The Netherlands.

Hatta, N., Fujimoto, H. and Takuda, H. (1995), "Deformation process of a water droplet impinging on a solid surface", *J. Fluids. Eng.*, Vol. 117, pp. 394-401.

Hatta, N., Fujimoto, H., Kinoshita, K. and Takuda, H. (1997), "Experimental study of deformation mechanism of a water droplet impinging on hot metallic surfaces above the Leidenfrost temperatre", *J. Fluids. Eng.*, Vol. 119, pp. 692-704.

Hernandez, J.P. (1999), "Reciprocidad Dual y Elementos de Frontera para Fluidos Newtonianos y No Newtonianos en Tres Dimensiones", Thesis, Mechanical Engineering Department, Universidad Pontificia Bolivariana, Medellin, Colombia.

Ladyzhenskaya, O.A. (1963), *The Mathematical Theory of Viscous Incompressible Flow*, Gordon and Breach, New York.

Liao, S. (1997), "Boundary element method for general nonlinear differential operators", *Eng. Anal. Bound. Elem.*, Vol. 20, pp. 91-9.

Nardini, D. and Brebbia, C.A. (1982), "A new approach to free vibration analysis using boundary elements", *BEM IV*, Computational Mechanics Publications, Southampton.

Partridge, P.W. (1997), "Approximation functions in the dual reciprocity method", *Boundary Elements Communications*, Vol. 8 No. 1, pp. 1-5.

Partridge, P.W. (2000), "Towards criteria for selecting approximation functions in the dual reciprocity method", *Eng. Anal. Bound. Elem.*, Vol. 24, pp. 519-29.

Partridge, P.W., Brebbia, C.A. and Wrobel, L.C. (1991), *The Dual Reciprocity Boundary Element Method*, Computational Mechanics Publications, Southampton.

Passandideh-Fard, M., Qiao, Y.M., Chandra, S. and Mostaghimi, J. (1996), "Capillary effects during droplet impact on a solid surface", *Phys. Fluids.*, Vol. 8 No. 3, pp. 650-9.

Power, H. (1996), "A second kind integral equation formulation for the low Reynolds number interaction between a solid particle and a viscous drop", *J. Eng. Math.*, Vol. 30, pp. 225-37.

Power, H. and Mingo, R. (2000), "The DRM subdomain decomposition approach to solve the two-dimensional Navier-Stokes system of equations", *Eng. Anal. Bound. Elem.*, Vol. 24, pp. 121-8.

Power, H. and Partridge, P.W. (1994), "The use of the Stokes fundamental solution for the boundary only formulation of the three dimensional Navier-Stokes equations for moderate Reynolds Numbers", *Int. J. Num. Meth. Eng.*, Vol. 37, pp. 1825-40.

Power, H. and Wrobel, L.C. (1995), *Boundary Integral Methods in Fluid Mechanics*, Computational Mechanics Publications, Southampton.

Pozrikidis, C. (1990), "The deformation of a liquid drop moving normal to a plane wall", *J. Fluid Mech.*, Vol. 215, pp. 331-63.

Pozrikidis, C. (1992), *Boundary Integral and Singularity Methods for Linearized Viscous Flow*, Cambridge University Press, New York.

Primo, A.R.M., Wrobel, L.C. and Power, H. (2000), "Boundary integral formulation for slow viscous flow in a deforming region containing a solid inclusion", *Eng. Anal. Bound. Elem.*, Vol. 24, pp. 53-63.

Rallison, J.M. and Acrivos, A. (1978), "A numerical study of the deformation and burst of a viscous drop in an extensional flow", *J. Fluid Mech.*, Vol. 89 No. 1, pp. 191-200.

Rallison, J.M. and Acrivos, A. (1984), "The deformation of small viscous drops and bubbles in shear flows", *Ann. Rev. Fluid Mech.*, Vol. 16, pp. 45-66.

Rios, A.C. (1999), "Simulation of mixing in single screw extrusion using the boundary integral method", PhD Thesis, University of Wisconsin-Madison.

Telles, J.C. (1987), "A self-adaptive coordinate transformation for efficient numerical evaluation of general boundary element integrals", *Int. J. Numer. Meth. Eng.*, Vol. 24, pp. 959-73.

Weiss, D.A. and Yarin, A.L. (1999), "Single drop impact onto liquids films: neck distortion, jetting, tiny bubble entrainment, and crown formation", *J. Fluid Mech.*, Vol. 385, pp. 229-54.

Wrobel, L.C. and Brebbia, C.A. (1987), "The dual reciprocity boundary element formulation for nonlinear diffusion problems", *Computer Methods in Applied Mechanics and Engineering*, Vol. 65, pp. 147-64.

Yarin, A.L. and Weiss, D.A. (1995), "Impact of drops on solids surfaces: self-similar capillary waves, and splashing as a new type of kinematic discontinuity", *J. Fluid Mech.*, Vol. 283, pp. 141-8.

Further reading

Davidson, M.R. (2000), "Boundary integral prediction of the spreading of an inviscid drop impacting on a solid surface", *Chemical Engineering Science*, Vol. 55, pp. 1159-70.

Davis, B.A., Florez, W.F. and Osswald, T.A. (1996), "Investigation of non-linear flows in polymer mixing", *BEM XVII*, Computational Mechanics Publications, New York, pp. 571-97.

Partridge, P.W. and Sensale, B. (1997), "Hybrid approximation functions in the dual reciprocity boundary element method", *Comm. Num. Meth. Eng.*, Vol. 13, pp. 83-94.

Power, H. and Partridge, P.W. (1993), "Dual reciprocity boundary element method for the time-dependent Stokes flow", *Int. J. Num. Meth. Heat Fluid Flow*, Vol. 3, pp. 145-55.

Rein, M. (1993), "Phenomena of liquid drop impact on solid and liquid surfaces", *Fluid Dyn. Res.*, Vol. 12, pp. 61-82.

Appendix. The particular solutions for the 2D non-homogeneous stokes flow

To find the solution of the non-homogeneous Stokes system of equations (20) and (21), the approach suggested by Happel and Brenner (1973) can be used. The tensor $\hat{u}_i^{lm}(\mathbf{x})$ is defined in terms of the potential ψ^m as follows,

$$\hat{u}_i^{lm}(\mathbf{x}) = \frac{\partial^2 \psi^m(\mathbf{x})}{\partial x_j \partial x_j}\delta_{il} - \frac{\partial^2 \psi^m(\mathbf{x})}{\partial x_i \partial x_l} \tag{46}$$

With the substitution of equation (46) into non-homogeneous Stokes flow, we will find a particular solution ψ^m if the following non-homogeneous bi-harmonic equation is satisfied,

$$\mu \frac{\partial^4 \psi^m(\mathbf{x})}{\partial x_j \partial x_j \partial x_j \partial x_j} = f^m(\mathbf{x}) \tag{47}$$

together with the equation,

$$\hat{p}^{lm}(\mathbf{x}) = -\mu \frac{\partial^3 \psi^m(\mathbf{x})}{\partial x_j \partial x_j \partial x_l} \tag{48}$$

According to Cheng (2000) the particular solution of the bi-harmonic operator (47) defined as,

$$\frac{\partial^4 \psi^m(\mathbf{x})}{\partial x_j \partial x_j \partial x_j \partial x_j} = r^{2n}\log(r) \quad n \geq 1 \text{ in } R^2 \tag{49}$$

is given by,

$$\psi^m(\mathbf{x}) = \frac{r^{2n+4}}{16(n+1)^2(n+2)^2}\left(\log(r) - \frac{2n+3}{(n+1)(n+2)}\right) \tag{50}$$

More specifically for the present work ($n = 1$),

$$\psi^m(\mathbf{x}) = \frac{r^6}{576}\left(\log(r) - \frac{5}{6}\right) \tag{51}$$

In a similar fashion the particular solution of the non-homogeneous bi-harmonic equation for the global functions $\{1, x_1, x_2\}$, that depend not on the Euclidean distance r, but only on the coordinates of the collocation node $x = (x_1, x_2)$, can be obtained (Cheng *et al.*, 1994). The results are summarized as follows,

$$\psi^m(\mathbf{x}) = \frac{|\mathbf{x}|^4}{64} \qquad \text{for } f^m(\mathbf{x}) = 1 \tag{52}$$

$$\psi^m(\mathbf{x}) = \frac{1}{2}\left(\frac{x_1^5}{120} + \frac{x_1^3 x_2^2}{24}\right) \qquad \text{for } f^m(\mathbf{x}) = x_1 \tag{53}$$

$$\psi^m(\mathbf{x}) = \frac{1}{2}\left(\frac{x_2^5}{120} + \frac{x_2^3 x_1^2}{24}\right) \qquad \text{for } f^m(\mathbf{x}) = x_2 \tag{54}$$

Thus, the particular solution for the velocity can be obtained from equation (47), and the tractions $\hat{t}_i^{lm}$ associated with it are defined as,

$$\hat{t}_i^{lm} = \hat{\sigma}_{ij} n_j \tag{55}$$

where

$$\hat{\sigma}_{ij} = -\hat{p}^{lm}\delta_{ij} + \mu\left(\frac{\partial \hat{u}_i^{lm}}{\partial x_j} + \frac{\partial \hat{u}_j^{lm}}{\partial x_i}\right) \tag{56}$$

With the procedure explained above, the particular solutions for the velocity are:

$$\hat{u}_i^{lm} = \frac{1}{96\mu}\left[\left(5r^4 \log r - \frac{7}{3}r^4\right)\delta_{il} - \hat{x}_i\hat{x}_l\left(4r^2 \log r - \frac{5}{3}r^2\right)\right] \tag{57}$$

for $f^m = r^2 \log r$ and $\hat{\mathbf{x}} = \mathbf{x} - \mathbf{x}^{\mathrm{m}}$.. On the other hand, for the global functions $f^m = \{1, x_1, x_2\}$ are,

$$\hat{u}_i^{lm} = \frac{1}{16\mu}(3|\mathbf{x}|^2\delta_{il} - 2x_i x_l) \tag{58}$$

$$\hat{u}_i^{lm} = \frac{1}{24\mu}\left[x_1^3(3\delta_{il} - 2\delta_{1l}\delta_{1i} - \delta_{2l}\delta_{2i}) + 3x_2^2 x_1(\delta_{il} - \delta_{1l}\delta_{1i}) - 3x_1^2 x_2(\delta_{1l}\delta_{2i} + \delta_{2l}\delta_{1i})\right] \tag{59}$$

and

$$\hat{u}_i^{lm} = \frac{1}{24\mu}\left[x_2^3(3\delta_{il} - 2\delta_{2l}\delta_{2i} - \delta_{1l}\delta_{1i}) + 3x_1^2 x_2(\delta_{il} - \delta_{2l}\delta_{2i}) - 3x_2^2 x_1(\delta_{1l}\delta_{2i} + \delta_{2l}\delta_{1i})\right], \tag{60}$$

respectively. Similar expressions are deduced for the tractions,

$$\hat{t}_i^{lm} = \frac{1}{96}\left[8r^2(\hat{x}_i n_l + \hat{x}_j n_j \delta_{il} + \hat{x}_l n_i)(2\log r - 1/3) - 4\hat{x}_i\hat{x}_l\hat{x}_j n_j(4\log r + 1/3)\right] \tag{61}$$

for $f^m = r^2 \log r$,, and

$$\hat{t}_i^{lm} = \frac{1}{4}\left[x_i n_l + x_j n_j \delta_{il} + x_l n_i\right] \tag{62}$$

$$\hat{t}_i^{lm} = \frac{1}{8}\{x_1^2\big[3(n_1\delta_{il} + n_l\delta_{1i} + n_i\delta_{1l}) - 2(2n_1\delta_{1i}\delta_{1l} + n_1\delta_{2i}\delta_{2l} + n_2\delta_{1i}\delta_{2l} + n_2\delta_{1l}\delta_{2i})\big]$$
$$+x_2^2\big[n_1\delta_{il} + n_l\delta_{1i} + n_i\delta_{1l} - 2n_1\delta_{1i}\delta_{1l}\big] + 2x_1x_2(n_2\delta_{il} + n_l\delta_{2i} + n_i\delta_{2l}) \quad (63)$$
$$-4x_1x_2(n_2\delta_{1i}\delta_{1l} + n_1\delta_{1i}\delta_{2l} + n_1\delta_{1l}\delta_{2i})\}$$

and

$$\hat{t}_i^{lm} = \frac{1}{8}\{x_2^2\big[3(n_2\delta_{il} + n_l\delta_{2i} + n_i\delta_{2l}) - 2(2n_2\delta_{2i}\delta_{2l} + n_2\delta_{1i}\delta_{1l} + n_1\delta_{2i}\delta_{1l} + n_1\delta_{2l}\delta_{1i})\big]$$
$$+x_1^2\big[n_2\delta_{il} + n_l\delta_{2i} + n_i\delta_{2l} - 2n_2\delta_{2i}\delta_{2l}\big] + 2x_1x_2(n_1\delta_{il} + n_l\delta_{1i} + n_i\delta_{1l}) \quad (64)$$
$$-4x_1x_2(n_2\delta_{2i}\delta_{1l} + n_1\delta_{2i}\delta_{2l} + n_2\delta_{2l}\delta_{1i})\}$$

for $f^m = \{1, x_1, x_2\}$, respectively.